The S5–S6 Linker of Repeat I Is a Critical Determinant of L-Type Ca^{2+} Channel Conductance

Robert T. Dirksen, Junichi Nakai, Adom Gonzalez, Keiji Imoto,* and Kurt G. Beam
Department of Anatomy and Neurobiology, College of Veterinary Medicine and Biomedical Sciences, Colorado State University, Fort Collins, Colorado 80523 USA, and *Department of Information Physiology, National Institute for Physiological Sciences, Myodaiji-cho, Okazaki 444, Japan

ABSTRACT The α_1-subunits of the skeletal and cardiac L-type calcium channels (L-channels) contain nearly identical pore regions (P-regions) in each of the four internal homology repeats. In spite of this high conservation of the P-regions, native skeletal L-channels exhibit a unitary conductance that is only about half that of native cardiac L-channels. To identify structural determinants of this difference in L-channel conductance, we have characterized unitary activity in cell-attached patches of dysgenic myotubes expressing skeletal, cardiac, and chimeric L-channel α_1-subunits. Our results demonstrate that the S5–S6 linker of repeat I (IS5–IS6 linker) is a critical determinant of the difference in skeletal and cardiac unitary conductance. The unitary conductances attributable to the wild-type skeletal (CAC6; ~14 pS) and cardiac (CARD1; ~25 pS) α_1-subunits expressed in dysgenic myotubes are identical to those observed in native tissues. Chimeric α_1-subunits containing skeletal sequence for the first internal repeat and all of the putative intracellular loops (SkC15), the IS5–IS6 linker and the intracellular loops (SkC51), or only the IS5–IS6 linker (SkC49) each exhibit a low, skeletal-like unitary conductance (≤17 pS). Constructs in which the IS5–IS6 linker is of cardiac origin (CARD1 and CSk9) display cardiac-like conductance (~25 pS). Unitary conductance and the rate of channel activation are apparently independent processes, since both SkC51 and SkC49 exhibit low, skeletal-like conductance and rapid, cardiac-like rates of ensemble activation. These results demonstrate that the IS5–IS6 linker strongly influences the single channel conductance of L-channels in a manner that is independent from the rate of channel activation.

INTRODUCTION

L-type calcium channels (L-channels) from endocrine, cardiac, and smooth muscle cells exhibit very similar high rates of calcium permeation (i.e., conductance) that appear to be intrinsic properties of the pore-forming calcium channel α_1-subunits (Gollasch et al., 1996). The large conductance of these L-channels has been suggested to involve negative charges within the external mouth of the channel, which increase the concentration of charge carrier just outside the entrance to the pore (Gollasch et al., 1996). The conservation of large conductance of L-channels from these different tissues emphasizes the importance of calcium permeation through these channels for processes as diverse as secretion and contraction of cardiac and smooth muscle. Interestingly, skeletal L-channels exhibit a substantially reduced unitary conductance (Dirksen and Beam, 1995) and calcium entry through these L-channels is not required for contraction of skeletal muscle (Armstrong et al., 1972).

The α_1-subunits of the skeletal and cardiac L-channels (also termed dihydropyridine receptors, DHPRs) are highly homologous proteins, exhibiting an 80% similarity at the amino acid level (Fujita et al., 1993). Nevertheless, skeletal and cardiac L-channels differ with regard to their functions in excitation-contraction coupling, rates of channel activation and inactivation, and unitary channel conductance (as mentioned above). Chimeric mutagenesis studies of skeletal and cardiac DHPRs have revealed that the intracellular loop connecting repeats II and III is critical for skeletal-type excitation-contraction coupling (Tanabe et al., 1990a), and that the S3 segment and the linker connecting the S3–S4 segments of repeat I strongly influences the rate of channel activation (Nakai et al., 1994). However, there have been no systematic studies aimed at identifying the regions that cause the cardiac DHPR to exhibit a much larger conductance than its skeletal homolog (25 pS versus 14 pS, under comparable experimental conditions; Dirksen and Beam, 1995, 1996; Reuter et al., 1982).

Ion selectivity and permeability of voltage-dependent ion channels are greatly influenced by a specific group of amino acids found in the S5–S6 linkers. These amino acids constitute the pore regions (P-regions), which are thought to contribute to the formation of the ion permeation pathway (Yellen et al., 1991). In calcium channels, four glutamate residues (one in each of the four P-regions) are necessary for high-affinity (μM) calcium binding within the channel pore and, thus, critically influence selectivity and permeation (Yang et al., 1993). The importance of the P-regions is emphasized by the fact that they are nearly identical in the skeletal and cardiac L-channels (in each of the four repeats,

Received for publication 14 April 1997 and in final form 2 June 1997.

Address reprint requests to Dr. Kurt G. Beam, Department of Anatomy and Neurobiology, College of Veterinary Medicine and Biomedical Sciences, Colorado State University, Fort Collins, CO 80523. Tel.: (970) 491-1566; Fax: (970) 491-7907; E-mail: kbeam@vines.colostate.edu.

Dr. Nakai's and Dr. Imoto's present address is Department of Information Physiology, National Institute for Physiological Sciences, Myodaiji-cho, Okazaki 444, Japan.

Dr. Gonzalez's present address is the Department of Molecular Biophysics/Physiology, Rush University, 1750 W. Harrison St., Chicago, IL 60612.

0006-3495/97/09/1402/08 $2.00

there are 11 identical residues and one conservative substitution between the skeletal and cardiac P-regions). This high sequence similarity of the P-regions suggests that amino acids outside the P-region may be crucial for the difference in skeletal and cardiac unitary conductance. We have investigated the single channel conductance of a series of chimeric L-channel α_1-subunits expressed in dysgenic myotubes. Our results reveal that the IS5–IS6 linker is a critical determinant of L-channel unitary conductance and suggests that amino acids within or adjacent to the P-region of the first repeat impart a strong influence on ion flux through the channel.

METHODS

Preparation of cells

Primary cultures of normal and dysgenic myotubes were prepared from newborn mice as described previously (Beam and Knudson, 1988; Tanabe et al., 1988). All experiments were performed 7–11 days after the initial plating of myoblasts and were carried out at room temperature (20–22°C).

Construction of DHPR cDNA

The construction and composition of SkC15 (Tanabe et al., 1991) and CSk9 (Tanabe et al., 1990b) were as described previously. The compositions of SkC51 and SkC49 are given below [Sk and C skeletal muscle (Tanabe et al., 1987), and cardiac muscle (Mikami et al., 1989) DHPR, respectively; numbers in parentheses are amino acid numbers; for a region of identical sequence, amino acid numbers are given as if the entire region were of cardiac sequence]: SkC51 Sk(1–55), C(159–320), Sk(219–309), C(411–464), Sk(364–448), C(571–787), Sk(666–791), C(923–1204), Sk(1074–1129), C(1261–1634), and Sk(1510–1873). SkC49 C(1–320), Sk(219–309), and C(411–2171). To construct SkC51, a PCR product was amplified from CSk9 using M51A and M51B primers (primers defined below). A final PCR was performed with pCAC6 and the M51A-M51B PCR product as templates using S4–15 and M51B as primers. The *Sac*I-*Pst*I fragment from the final PCR product was inserted into pBluescript SK(-) (Stratagene, LaJolla, CA) and sequenced to yield pBS51a. The following restriction fragments were ligated together to yield pSkC51: *Sac*I(Sk651)-*Pst*I(C1833) from pBS51a, the *Pst*I(C1833)-BstBI(Sk2175), BstBI(Sk2175)-*Sal*I(vector), and *Sal*I(vector)-*Sac*I(C957) fragments from pSkC15. Primers used were S4–15(forward): Sk378–394; M51A(forward): Sk909–927, C1231–1250; and M51B(reverse): C1813–1835. The *Sac*I(Sk651)-*Bam*HI(C1265) fragment from pSkC51, and the *Bam*HI(C265)-*Afl*II(C2690), *Afl*II(C2690)-*Sal*I(vector), and *Sal*I(vector)-*Sac*I(C957) fragments from pCARD1 were ligated together to yield pSkC49.

Injection of expression plasmids

On the sixth or seventh day after the initial plating of myoblasts into primary culture, nuclei of dysgenic myotubes within demarcated regions of 35-mm culture dishes were microinjected (Tanabe et al., 1988) with expression plasmids (0.2–1.0 $\mu g/\mu l$) carrying cDNA inserts encoding either the skeletal DHPR, CAC6 (Tanabe et al., 1987), the cardiac DHPR, CARD1 (16), or one of the chimeric DHPRs (SkC15, CSk9, SkC51, or SkC49). Myotubes were tested for electrically evoked contractions 1–4 days after injection to identify those expressing the injected cDNA (Tanabe et al., 1988).

Single channel measurements

Unitary calcium channel currents were measured using the cell-attached mode of the patch clamp technique (Hamill et al., 1981) as described previously (Dirksen and Beam, 1995, 1996). Fire-polished borosilicate pipettes were coated with Sylgard (Dow-Corning, Midland, MI) and had resistances of 2–4 MΩ when filled with the pipette solution. Currents were acquired with an EPC-7 (Medical Systems, Greenvale, NY) or Dagan 3900A (Dagan Corporation, Minneapolis, MN) patch clamp amplifier, filtered at 1 kHz with an 8-pole Bessel filter (Frequency Devices, Haverhill, MA), and acquired at 10 kHz using an IDA Interface (INDEC Systems, Capitola, CA). Data were collected using the Basic-Fastlab (INDEC Systems, Capitola, CA) software and analyzed using a combination of pCLAMP (Axon Instruments, Foster City, CA) and an analysis program kindly provided by Dr. Don Campbell.

Records of channel activity were digitally corrected for leak and capacitative currents by subtracting from each record either the average of multiple sweeps without channel openings (null sweeps) or a multiexponential curve that had been fitted to a null sweep. Ensemble averages were compiled by averaging all leak-subtracted current records in a series. The potential across the patch membrane was calculated as described previously (Fujita et al., 1993; Dirksen and Beam, 1995, 1996). Mean open current amplitudes were determined from Gaussian fits of either all-point current amplitude histograms or amplitude histograms of single open events. Openings to an apparent subconductance level were occasionally present for some constructs, but were not studied further since they were neither consistently observed nor did they contribute significantly to amplitude histograms.

The activation phase of ensemble currents was fitted by the following exponential function:

$$I(t) = I_\infty[1 - \exp(-t/\tau_{act})]$$

where $I(t)$ is the current at time t after the depolarization, I_∞ is the steady-state current, and τ_{act} is the time constant of activation.

Solutions

Myotubes were bathed in a normal rodent Ringer's solution consisting of (mM): 145 NaCl, 5 KCl, 2 $CaCl_2$, 1 $MgCl_2$, and 10 HEPES (pH = 7.40 with NaOH). Cell-attached patch pipettes contained (in mM): 110 $BaCl_2$, 0.003 tetrodotoxin, 0.005 (±) Bay K 8644 (kindly supplied by Dr. A. Scriabine, Miles Laboratories, Inc., New Haven, CT), and 10 HEPES (pH = 7.40 with TEA-OH).

RESULTS

Fig. 1 shows unitary and ensemble activity of L-channels in cell-attached patches obtained from a normal myotube (normal, *left*) and dysgenic myotubes that were injected with cDNA plasmids encoding either the rabbit skeletal muscle DHPR (CAC6, *center*) or a chimeric DHPR in which repeat I and the putative intracellular domains were of skeletal origin, and repeats II–IV were of cardiac origin (SkC15, *right*). Representative leak-subtracted sweeps at three different potentials (−10, 0, and 10 mV) are shown for each experiment. For all three patches, the channels displayed similar, low, unitary conductances (ranging from 14.3 pS to 16.8 pS) and a slowly activating ensemble current at +10 mV (*bottom*). Since SkC15 channels displayed both slow activation and a small unitary conductance, repeat I appeared not only to have an important influence on the rate of channel activation (Nakai et al., 1994; Tanabe et al., 1991), but also on ion permeation. However, since the intracellular domains of SkC15 are also of skeletal origin, they could conceivably have played a role in ion permeation.

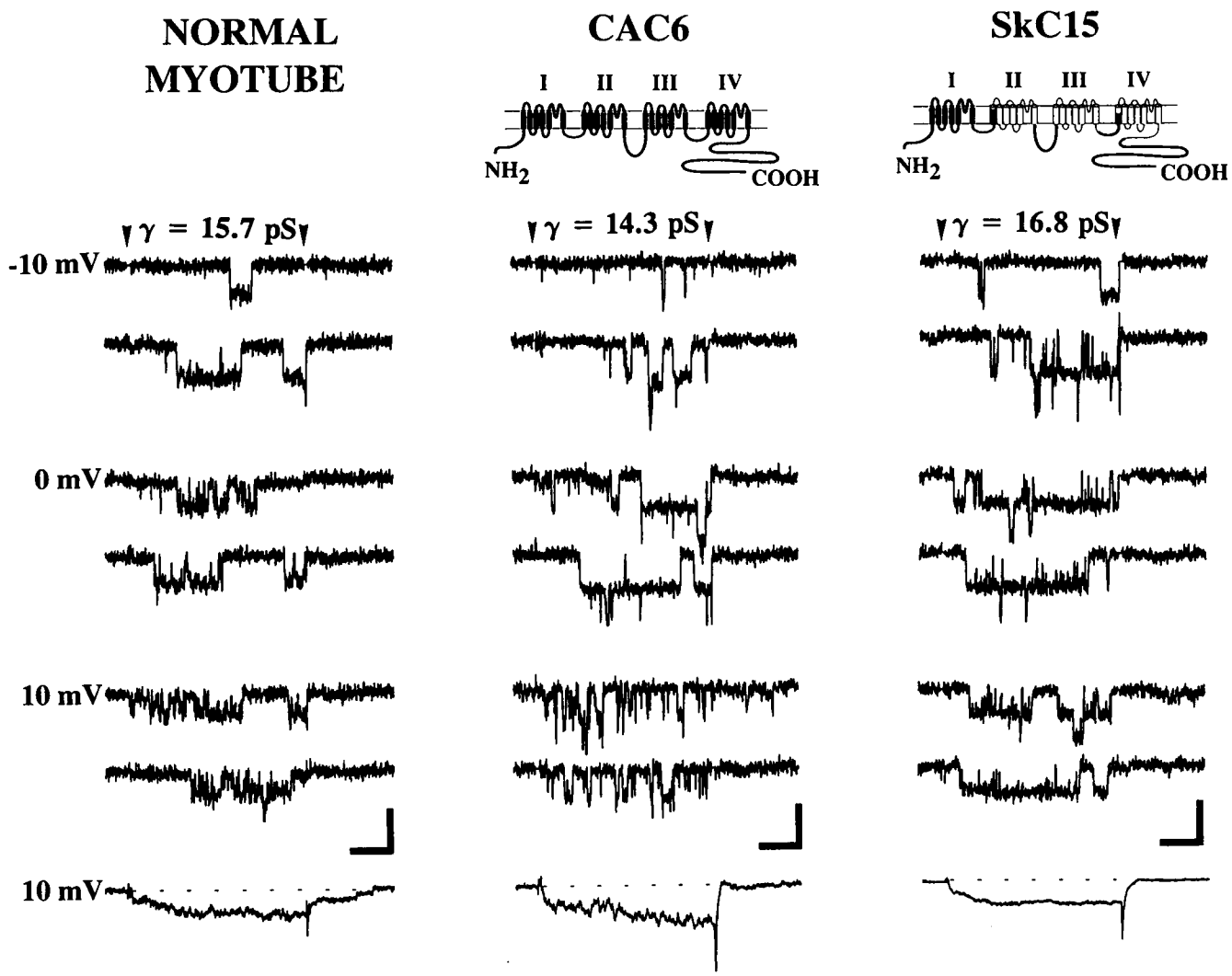

FIGURE 1 Unitary activity of channels displaying slow ensemble activation. Cell-attached patches were obtained from a normal myotube (*left*, 3-channel patch) and dysgenic myotubes expressing either CAC6 (*center*, 4-channel patch) or SkC15 (*right*, 4-channel patch). Schematic representations are shown for CAC6 and SkC15, with thick lines and filled cylinders representing regions of skeletal origin and thin lines and hollow cylinders representing regions of cardiac origin. Representative, leak-subtracted sweeps are shown for each experiment (with 110 mM Ba^{2+} as charge carrier) at three different potentials (−10, 0, and 10 mV). For this and all subsequent figures, downward current deflections represent channel open events, arrowheads indicate when the test depolarizations began and ended, and the single channel conductance (γ) calculated for each experiment is shown above the set of sweeps of unitary activity. (*Bottom*) Ensemble averages (at +10 mV) of 40 (normal), 25 (CAC6), and 54 (SkC15) sweeps. Ensembles of each construct exhibit slow activation (τ_{act} > 10 ms). Calibrations: horizontal = 50 ms for both unitary and ensemble traces; vertical = 1.0 pA for unitary traces and 0.3 pA (normal), 0.6 pA (CAC6), and 1.2 pA (SkC15) for ensemble traces. The dotted line represents the zero current level.

We investigated the possible role of the intracellular domains and the linker between the S5 and S6 segments of repeat I (IS5–IS6 linker) on ion permeation in experiments of the sort shown in Fig. 2. Fig. 2 compares single channel and ensemble traces from dysgenic myotubes expressing the purely cardiac DHPR (CARD1, *left*), or the chimeric DHPRs CSk9 (*center*), and SkC51 (*right*). CSk9 is like SkC15 in having the putative intracellular domains of skeletal origin, but differs in that *all four* repeats are of cardiac origin. SkC51 is identical to CSk9 except that the IS5–IS6 linker of SkC51 has a skeletal sequence. Ensembles for all three constructs (Fig. 2, *bottom*) activated ~5 times faster than those for CAC6, SkC15, or normal myotubes. As expected, CARD1 unitary activity yielded a large, single channel conductance (26.4 pS) similar to that observed in native cardiac myocytes (~25 pS in 110 mM Ba^{2+}; Reuter et al., 1982). CSk9 also exhibited a cardiac-like conductance (23.8 pS). The cardiac-like conductance of CSk9 indicates that a skeletal sequence for the intracellular domains alone is insufficient to account for the low, skeletal-like conductance of SkC15. For SkC51, the IS5–IS6 linker of CSk9 was converted to skeletal sequence. This alteration was sufficient to yield a chimeric DHPR (SkC51), which displays rapid activation like the cardiac DHPR, yet a small unitary

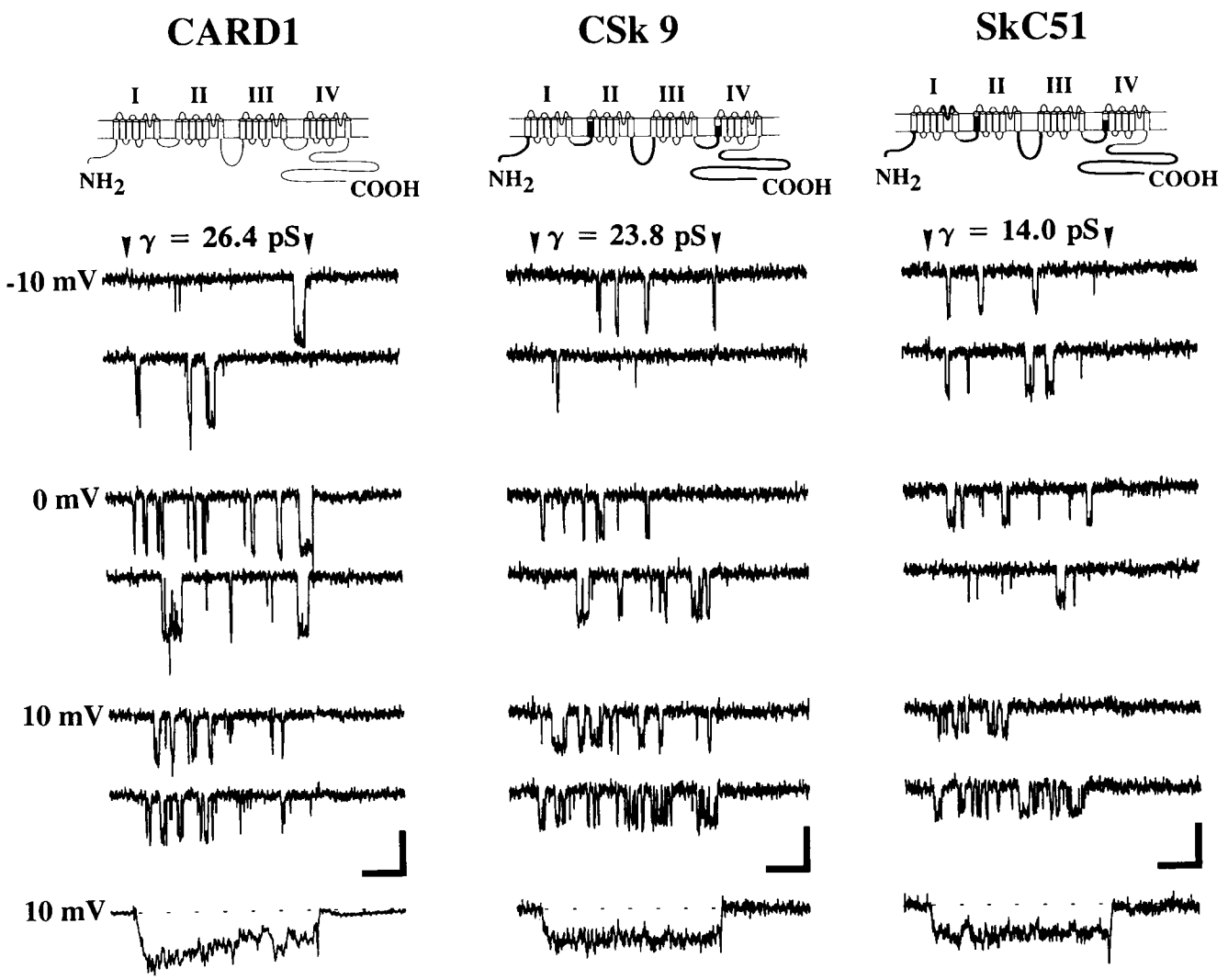

FIGURE 2 Unitary activity of rapidly activating L-channels. Cell-attached patches obtained from dysgenic myotubes expressing either CARD1 (*left*, 3-channel patch), CSk9 (*center*, 2-channel patch), or SkC51 (*right*, 1-channel patch). Representative, leak-subtracted sweeps at three different potentials (−10, 0, and 10 mV) are shown for each experiment. (*Bottom*) Ensemble averages (at +10 mV) of 40 (CARD1), 120 (CSk9), and 80 (SkC51) sweeps. Ensembles of each construct exhibit rapid (τ_{act} < 10 ms) activation. Calibrations: horizontal = 50 ms for both unitary and ensemble traces; vertical = 1.0 pA for unitary traces and 0.8 pA (normal), 0.2 pA (CAC6), and 0.2 pA (SkC15) for ensemble traces.

conductance like that of the purely skeletal DHPR. Thus, these data demonstrate that the IS5–IS6 linker is a critical determinant of L-channel unitary conductance.

In order to establish more clearly a definitive role of the IS5–IS6 linker in the difference between skeletal and cardiac unitary conductance, we evaluated the single channel conductance of a final construct, SkC49 (Fig. 3). SkC49 is entirely cardiac in origin, except for skeletal sequence for the IS5–IS6 linker (see schematic in Fig. 3 *A*). The presence of any skeletal sequence in this small region (~4% of the entire protein) was sufficient to greatly reduce the unitary conductance of the cardiac L-type calcium channel (from 24.6 pS to 17.0 pS). Thus, from our experiments, the IS5–IS6 linker represents a primary determinant of the difference in the unitary conductance of skeletal and cardiac L-type calcium channels.

Plots of the average, single channel current amplitude versus voltage (*i-V*) relationships for the seven different L-channels studied in Figs. 1–3 are shown in Fig. 3 *B*. Open channel current levels were determined as described in Methods, and data sets were fitted by linear regressions. Each data point is the average (±SEM) of 5–9 individual experiments. As reported previously (Dirksen and Beam, 1995), L-channels in normal myotubes (●) exhibited a single channel conductance of ~14 pS. L-channels in dysgenic myotubes expressing CAC6 (■), SkC15 (▲), SkC51 (▼), or SkC49 (◆) exhibited similar low unitary conductances, ranging from 14.3 pS to 17.0 pS. On the other hand, CARD1 (□) and CSk9 (△) exhibited large single channel conductances (24.6 pS and 23.7 pS, respectively). The DHPR in normal myotubes, and each of the four DHPR constructs with skeletal sequence for the IS5–IS6 linker

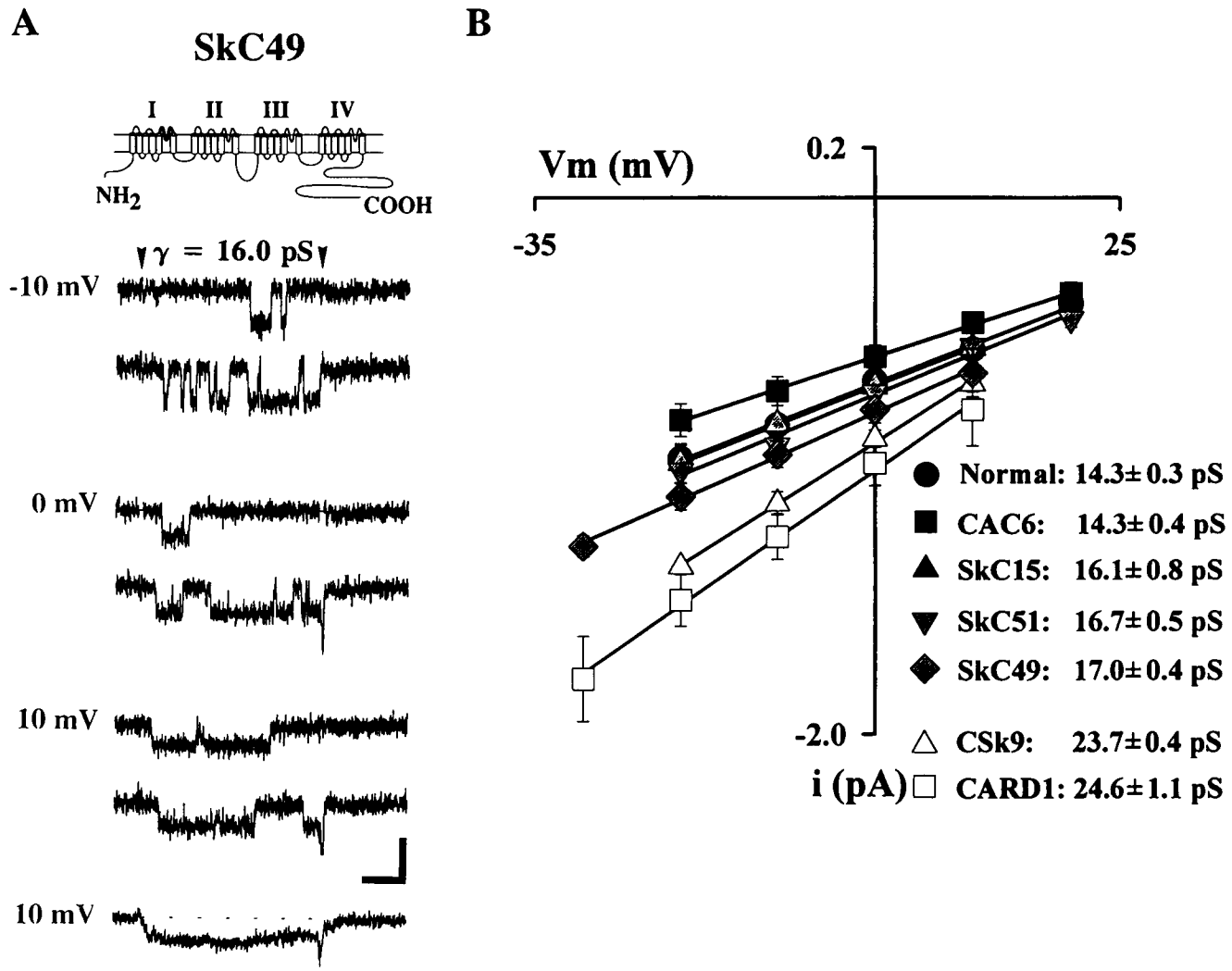

FIGURE 3 The IS5–IS6 linker is a critical determinant of L-channel conductance. (*A*) Cell-attached patch obtained from a dysgenic myotube expressing SkC49 (1-channel patch). Schematic representation shows that SkC49 is entirely of cardiac origin, except for skeletal sequence for the IS5–IS6 linker. Representative, leak-subtracted sweeps are shown for three different potentials (−10, 0, and 10 mV) for SkC49. (*Bottom*) Ensemble average (at +10 mV) of 40 sweeps of unitary activity. Note that SkC49 exhibited rapid, cardiac-like activation (τ_{act} < 10 ms) and a low, skeletal-like unitary conductance (16.0 pS). Calibrations: horizontal = 50 ms for both unitary and ensemble traces; vertical = 1.0 pA for unitary traces and 0.3 pA for the ensemble trace. (*B*) Single channel current versus voltage relationships for slowly and rapidly activating L-channels. Average (±SEM) single channel current versus voltage relationship tabulated from a total of 5–9 different experiments (≤4 channels per patch) for each channel type. Filled symbols represent constructs exhibiting the low, skeletal-like conductance (●, normal, n = 9; ■, CAC6, n = 9; ▲, SkC15, n = 9; ▼, SkC51, n = 7; and ◆, SkC49, n = 6) and open symbols represent constructs exhibiting the large, cardiac-like conductance (△, CSk9, n = 5 and □, CARD1, n = 9). The solid lines through the data points are linear regressions fitted to each data set (R^2 > 0.996 for each data set). Slope conductances (*inset*) were calculated as the arithmetic mean value for each construct. The conductance values of SkC15, SkC51, and SkC49 were statistically different (two-tailed, unpaired Student's t-test) from the conductance values of normal myotubes and dysgenic myotubes expressing CAC6 at a moderate confidence level ($0.0001 \leq p < 0.05$). Conductance values of normal myotubes and dysgenic myotubes expressing CAC6, SkC15, SkC51, and SkC49 were statistically different (two-tailed, unpaired Student's t-test) from those values of CSk9 and CARD1 at a very high confidence level ($p \ll 0.0001$). No other statistically significant differences were found among these data sets.

(CAC6, SkC15, SkC51, and SkC49), exhibited unitary conductances that differed from those attributable to CSk9 and CARD1, at a very high confidence level ($p \ll 0.0001$). Since CAC6, SkC15, SkC51, and SkC49 have skeletal sequence in common only for the IS5–IS6 linker, this region appears to have an important role in the difference in the magnitude of open channel ion flux mediated by skeletal and cardiac L-channels. To further test the importance of the IS5–IS6 linker on the difference in skeletal and cardiac unitary conductance, we measured unitary currents mediated by SkC11 (Tanabe et al., 1991), which contains a cardiac sequence for the first repeat in an otherwise entirely skeletal channel. SkC11 channels exhibited cardiac-like conductance (24.4 ± 1.0 pS, n = 3) indicating that skeletal sequence in the P-regions of repeats II–IV is insufficient to account for low skeletal unitary conductance. Activation

rate and unitary conductance are evidently distinct and independent properties of the L-channel α_1-subunit, since SkC51 and SkC49 exhibit cardiac-like activation and skeletal-like conductance. This conclusion is further supported by the behavior of SkC47 (Nakai et al., 1994), which is entirely cardiac in origin except for having a skeletal sequence in IS3 and the IS3–IS4 linker. This construct displays skeletal-like, ensemble activation and cardiac-like, unitary conductance (data not shown).

DISCUSSION

The results presented in Figs. 1–3 show that the IS5–IS6 linker plays an important role in the difference in unitary conductance of cardiac and skeletal L-channels. This is shown most strikingly in the comparison of CARD1 and SkC49. CARD1 channel activity is characterized by rapid ensemble activation and a large unitary conductance. Simply substituting skeletal sequence for the IS5–IS6 linker in CARD1 results in a rapidly activating, low-conductance L-channel (SkC49). Thus, this minimal alteration is sufficient to dramatically reduce the cardiac single channel conductance independent of the rate of channel activation. Although we found that the IS5–IS6 linker is the region whose identity (skeletal versus cardiac) has the predominant effect on unitary conductance, other regions also have a small effect since SkC15, SkC51, and SkC49 each exhibit a slightly larger unitary conductance (see legend to Fig. 3) than the wild-type channel (i.e., normal myotubes and CAC6). Thus, regions within repeats II, III, and IV (e.g., S5–S6 linkers) may contribute to the lower skeletal unitary conductance, albeit to a minimal extent compared to the IS5–IS6 linker. However, the precise roles of the S5–S6 linkers of repeats II–IV to the low, skeletal conductance will require replacing the S5–S6 linker in each of these repeats of the cardiac L-channels with the corresponding skeletal sequence.

Our results are in contrast to those of Parent et al. (1995) who concluded that the IS5–IS6 linker does not play a prominent role in determining L-channel conductance properties. Differences in experimental methodologies may, in part, account for this discrepancy. Parent et al. (1995) compared the channel properties (activation, inactivation, and unitary conductance) of the cardiac DHPR with a chimeric DHPR (SK1H3) in which the N-terminus and the first internal repeat contained skeletal sequence in an otherwise cardiac background. The two constructs were expressed in combination with the ancillary subunits α_{2b} and the brain/cardiac β_{2a} in *Xenopus* oocytes, rather than in a mammalian muscle expression system (i.e., dysgenic myotubes) containing the muscle β_1 and α_2 subunits. In addition, *Xenopus* oocytes also endogenously express a β-subunit (β_3), which is not found in skeletal muscle (Tareilus et al., 1997). These differences in expression paradigms greatly influence the properties of the resulting ionic currents. For example, in the experiments of Parent et al. (1995) the entirely cardiac L-current exhibits a slow component of activation not seen upon expression in dysgenic myotubes (Dirksen and Beam, 1996; Tanabe et al., 1990b). In addition, SK1H3 exhibits a prominent inactivation component that is not observed upon expression of the similar construct, SkC15, in dysgenic myotubes (Tanabe et al., 1991). Therefore, differences in expression systems and the presence of distinct auxiliary subunits may contribute to the dissimilarities between our results and those of Parent et al. (1995) in activation, inactivation, and unitary conductance.

How can we account for our observation that the identity of the S5–S6 linker in repeat I has the largest effect on unitary conductance? One possibility is that the geometric arrangement of the IS5–IS6 linker is such that it most strongly influences ion flux. As a precedent for this idea, it has been suggested that the four essential P-region glutamates are asymmetrically arranged within the cardiac calcium channel pore; this arrangement was postulated in order to account for the observation that mutations of the glutamate in repeat III have a much greater effect on ion selectivity and permeation than comparable mutations in the other three repeats (Yang et al., 1993). As an alternative to the idea that an asymmetrical arrangement of the S5–S6 linkers accounts for the disproportionate influence of repeat I on unitary conductance, it might simply be that cardiac and skeletal S5–S6 linkers have a much more divergent sequence in repeat I than in the other three repeats. Fig. 4 compares the sequence of the skeletal and cardiac IS5–IS6 linkers. Consistent with its critical role in ion selectivity, the P-region embedded within the IS5–IS6 linker differs little between the skeletal and cardiac DHPRs: of 12 amino acids, 11 are identical and the 12th is a conservative change in which a tyrosine in the skeletal P-region is substituted for a phenylalanine in the cardiac P-region. In each of the other three repeats, the skeletal and cardiac P-regions also are identical at 11 positions and have a conservative change at the 12th position. It is conceivable that the more bulky and hydrophilic tyrosine residue in the skeletal repeat I P-region reduces ion flux through the skeletal L-channel. For example, the phenolic hydroxyl of tyrosine might impart a strong effect on ion conductance due to its hydrogen-bonding capability and proximity to the P-region glutamate residues. The potential importance of this phenylalanine residue is highlighted by the fact that a phenylalanine is also found at the second position of the P-regions of repeats II, III, and IV of both the skeletal and cardiac DHPRs. More definitive conclusions regarding this residue in repeat I will require determining the functional consequences of mutating the skeletal tyrosine residue to a phenylalanine. If the tyrosine residue in repeat I is found to confer the low skeletal conductance, then it will also be important to determine the effects of substituting a tyrosine for the conserved phenylalanines at the corresponding positions in repeats II–IV.

Due to the conservative nature of the single amino acid difference in the repeat I P-region, it is worth considering the possible role of divergence of the IS5–IS6 linker outside of the P-region to account for the difference in skeletal and

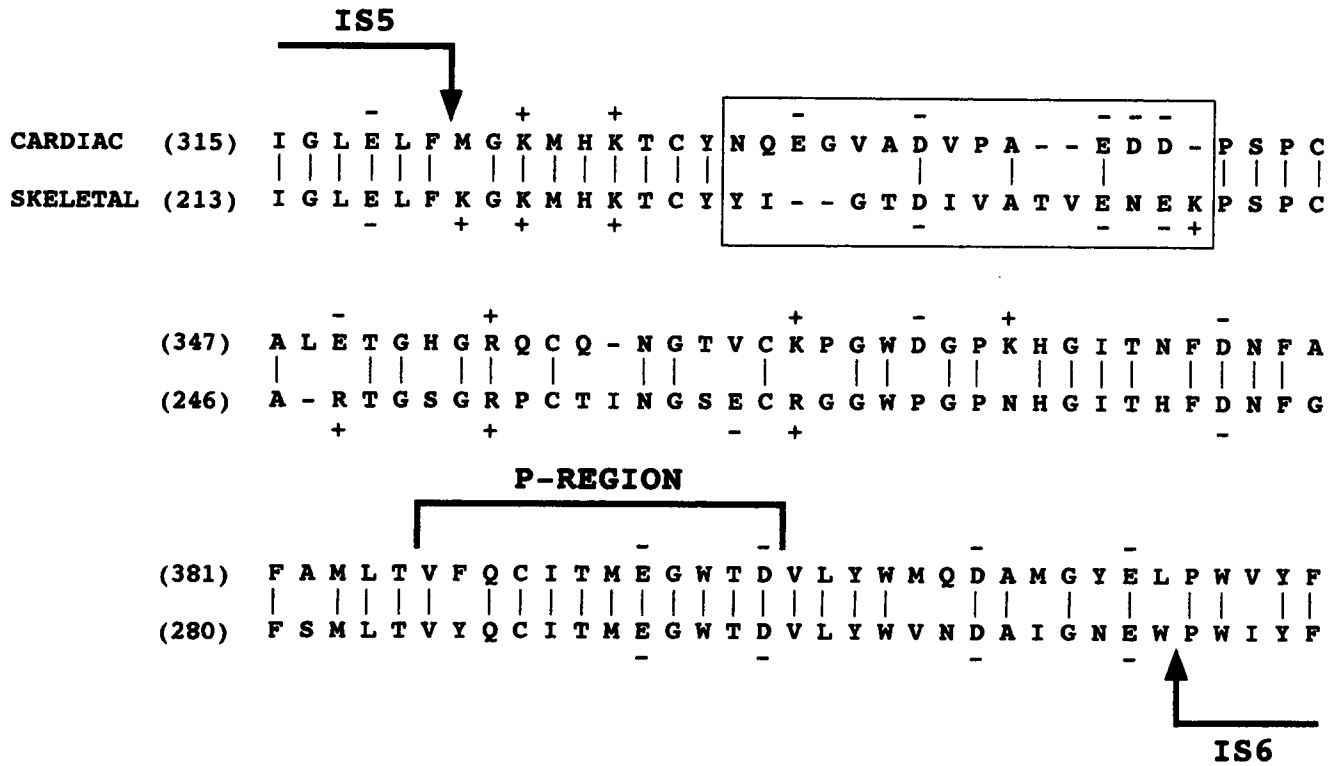

FIGURE 4 Comparison of the IS5–IS6 linker regions (one-letter amino acid code) of the skeletal (Tanabe et al., 1987) and cardiac (Mikami et al., 1989) DHPRs. The region between the arrowheads is of skeletal origin in SkC49. Between the paired sequences, vertical lines represent identical amino acids, dashes represent gaps introduced to maximally align the sequences, and the bracketed region represents the putative pore region (P-region) of the first repeat (Mikami et al., 1989). The numbers in parentheses represent the amino acid number of the first amino acid of each line. A "+" and "−" denote positively and negatively charged residues, respectively. The skeletal and cardiac IS5–IS6 linkers have net charges of −2 and −7, respectively. The majority of this difference is found in a small region of extremely low homology (*boxed region*) between the two DHPRs.

cardiac unitary conductance. In comparison to the highly conserved nature of the P-regions, the remaining portions of the S5–S6 linkers of each of the four repeats are less well conserved between skeletal and cardiac DHPRs. The non-P-region, flanking segments of the S5–S6 linkers of the skeletal and cardiac DHPRs, exhibit identity/similarity percentages of 64/78, 71/95, 62/73, and 71/84 in repeats I–IV, respectively (using the alignment of Fujita et al., 1993). If one compares the net charge of the S5–S6 linkers of the skeletal and cardiac L-channels, the first repeat shows the greatest difference. Specifically, the difference in the total net charge of the cardiac and skeletal S5–S6 linkers is −5 for repeat I and +1 for repeats II–IV. The majority of the excess negative charge of the cardiac IS5–IS6 linker occurs within a small region of very low homology to the skeletal IS5–IS6 linker (boxed region in Fig. 4). Interestingly, the human brain DHP-sensitive calcium channel (α_{1D}; Williams et al., 1992) has a IS5–IS6 linker similar to its cardiac counterpart in possessing both a phenylalanine at the second position in the P-region and a net charge difference of −5 compared to the skeletal IS5–IS6 linker (with the majority found in the boxed region of low homology depicted in Fig. 4). This may account for the cardiac-like conductance observed in GH_3 cells (Gollasch et al., 1996), which express both the α_{1C} and α_{1D} subunits (Birnbaumer et al., 1994).

A ring of negatively charged amino acids in the extracellular vestibule of sodium channels has been suggested to optimize conduction by electrostatic attraction of permeant cations to the sodium channel pore (Terlau et al., 1991). Thus, for the sodium channel, neutralization of even a single negatively charged residue within this ring is sufficient to dramatically reduce unitary conductance (Terlau et al., 1991; Noda et al., 1989). By analogy, it is tempting to speculate that the additional negative charges of the cardiac IS5–IS6 linker may be arranged in an extracellular vestibule so as to reduce the energy barrier for entry of permeant divalent cations into the pore. As an alternative to the idea that strictly electrostatic effects of the charged residues are the critical feature, it may be that the differences in amino acid sequence of the skeletal and cardiac IS5–IS6 region affect ion flux by altering the overall conformation of the pore. Alternatively, as pointed out above, differences with regard to the identity of the aromatic residue at the second position of the repeat I P-region provides an equally plausible mechanism for the lower unitary conductance of the skeletal L-channel. Point mutations in the charged residues of the IS5–IS6 linker and exchanging a phenylalanine for the tyrosine residue in the repeat I P-region will help to differentiate between these potential explanations.

We would like to thank Robin Morris, Kim Lopez-Jones, and Aaron Beam for excellent technical assistance.

This research was supported, in part, by the Ministry of Education, Science, Culture, and Sports of Japan, the Institute of Physical and Chemical Research, and National Institutes of Health Grant NS-24444 (to K.G.B.), and Postdoctoral Fellowship AR-08243 (to R.T.D.).

REFERENCES

Armstrong, C. M., F. M. Bezanilla, and P. Horowicz. 1972. Twitches in the presence of ethylene glycol bis(β-aminoethyl ether)-N-N′-tetraacetic acid. *Biochim. Biophys. Acta.* 267:605–608.

Beam, K. G., and C. M. Knudson. 1988. Calcium currents in embryonic and neonatal mammalian skeletal muscle. *J. Gen. Physiol.* 91:781–798.

Birnbaumer, L., K. P. Campbell, W. A. Catterall, M. M. Harpold, F. Hofmann, W. A. Horne, Y. Mori, A. Schwartz, T. P. Snutch, T. Tanabe, and R. W. Tsien. 1994. The naming of voltage-gated calcium channels. *Neuron.* 13:505–506.

Dirksen, R. T., and K. G. Beam. 1995. Single calcium channel behavior in native skeletal muscle. *J. Gen. Physiol.* 105:227–247.

Dirksen, R. T., and K. G. Beam. 1996. Unitary behavior of skeletal, cardiac, and chimeric L-type Ca^{2+} channels expressed in dysgenic myotubes. *J. Gen. Physiol.* 107:731–742.

Fujita, Y., M. Mynlieff, R. T. Dirksen, M.-S. Kim, T. Niidome, J. Nakai, T. Friedrich, N. Iwabe, T. Miyata, T. Furuichi, D. Furutama, K. Mikoshiba, Y. Mori, and K. G. Beam. 1993. Primary structure and functional expression of the Ω-conotoxin-sensitive N-type calcium channel from rabbit brain. *Neuron.* 10:585–598.

Gollasch, M., C. Ried, M. Liebold, H. Haller, F. Hofmann, and F. C. Luft. 1996. High permeation of L-type Ca^{2+} channels at physiological $[Ca^{2+}]$: homogeneity and dependence on the α_1-subunit. *Am. J. Physiol.* 271(*Cell Physiol.* 40):C842–C850.

Hamill, O. P., A. Marty, E. Neher, B. Sakmann, and F. J. Sigworth. 1981. Improved patch-clamp techniques for high-resolution current recording from cells and cell-free membrane patches. *Pflügers Arch.* 391:85–100.

Mikami, A., K. Imoto, T. Tanabe, T. Niidome, Y. Mori, H. Takeshima, S. Narumiya, and S. Numa. 1989. Primary structure and functional expression of the cardiac dihydropyridine-sensitive calcium channel. *Nature (London).* 340:230–233.

Nakai, J., B. A. Adams, K. Imoto, and K. G. Beam. 1994. Critical roles of the S3 segment and the S3–S4 linker of repeat I in activation of L-type calcium channels. *Proc. Natl. Acad. Sci. USA.* 91:1014–1018.

Noda, M., H. Suzuki, S. Numa, and W. Stühmer. 1989. A single point mutation confers tetrodotoxin and saxitoxin insensitivity on the sodium channel II. *FEBS Lett.* 259:213–216.

Parent, L., M. Gopalakrishna, A. E. Lacerda, X. Wei, and E. Perez-Reyes. 1995. Voltage-dependent inactivation in a cardiac-skeletal chimeric calcium channel. *FEBS Lett.* 360:144–150.

Reuter, H., C. F. Stevens, R. W. Tsien, and G. Yellen. 1982. Properties of single calcium channels in cardiac cell culture. *Nature (London).* 297: 501–504.

Tanabe, T., B. A. Adams, S. Numa, and K. G. Beam. 1991. Repeat I of the dihydropyridine receptor is critical in determining calcium channel activation kinetics. *Nature (London).* 352:800–803.

Tanabe, T., K. G. Beam, B. A. Adams, T. Niidome, and S. Numa. 1990a. Regions of the skeletal muscle dihydropyridine receptor critical for excitation-contraction coupling. *Nature (London).* 346:567–569.

Tanabe, T., K. G. Beam, J. A. Powell, and S. Numa. 1988. Restoration of excitation-contraction coupling and slow calcium current in dysgenic muscle by dihydropyridine receptor complementary DNA. *Nature (London).* 336:134–139.

Tanabe, T., A. Mikami, S. Numa, and K. G. Beam. 1990b. Cardiac-type excitation-contraction coupling in dysgenic muscle injected with cardiac dihydropyridine receptor cDNA. *Nature (London).* 344:451–453.

Tanabe, T., H. Takeshima, A. Mikami, V. Flockerzi, H. Takahashi, K. Kangawa, M. Kojima, H. Matsuo, T. Hirose, and S. Numa. 1987. Primary structure of the receptor for calcium channel blockers from skeletal muscle. *Nature (London).* 328:313–318.

Tareilus, E., M. Roux, N. Qin, R. Olcese, J. Zhou, E. Stefani, and L. Birnbaumer. 1997. A *Xenopus* oocyte β subunit: evidence for a role in the assembly/expression of voltage-gated calcium channels that is separate from its role as a regulatory subunit. *Proc. Natl. Acad. Sci. USA.* 94:1703–1708.

Terlau, H., S. H. Heinemann, W. Stühmer, M. Pusch, F. Conti, K. Imoto, and S. Numa. 1991. Mapping the site of block by tetrodotoxin and saxitoxin of sodium channel II. *FEBS Lett.* 293:93–96.

Williams, M. E., D. H. Feldman, A. F. McCue, R. Brenner, G. Velicelebi, S. B. Ellis, and M. M. Harpold. 1992. Structure and functional expression of α_1, α_2, and β subunits of a novel human neuronal calcium channel subtype. *Neuron.* 8:71–84.

Yang, J., P. T. Ellinor, W. A. Sather, J.-F. Zhang, and R. W. Tsien. 1993. Molecular determinants of Ca^{2+} selectivity and ion permeation in L-type Ca_{2+} channels. *Nature (London).* 366:158–161.

Yellen, G., M. E. Jurman, T. Abramson, and R. MacKinnon. 1991. Mutations affecting internal TEA blockade identify the probable pore-forming region of a K^+ channel. *Science.* 251:939–942.